

1 **SYNERGY BETWEEN SATELLITE OBSERVATIONS OF SOIL MOISTURE**
2 **AND WATER STORAGE ANOMALIES FOR ~~GLOBAL~~ RUNOFF**
3 **ESTIMATION**

4 Stefania Camici ⁽¹⁾, Gabriele Giuliani ⁽¹⁾, Luca Brocca ⁽¹⁾, Christian Massari ⁽¹⁾, Angelica Tarpanelli
5 ⁽¹⁾, Hassan Hashemi Farahani ⁽²⁾, Nico Sneeuw ⁽²⁾, Marco Restano ⁽³⁾, Jérôme Benveniste ⁽⁴⁾

6 *(1) National Research Council, Research Institute for Geo-Hydrological Protection, Perugia, Italy (s.camici@irpi.cnr.it)*

7 *(2) Institute of Geodesy, University of Stuttgart, Geschwister-Scholl-Straße 24D, 70174 Stuttgart, Germany*

8 *(3) SERCO c/o ESA-ESRIN, Largo Galileo Galilei, Frascati, 00044, Italy*

9 *(4) European Space Agency, ESA-ESRIN, Largo Galileo Galilei, Frascati, 00044, Italy*

10
11
12
13
14
15
16
17
18
19 **November 2020**

20 Submitted to:
21

* Correspondence to: Ph.D. Stefania Camici, Research Institute for Geo-Hydrological Protection, National Research Council, Via della Madonna Alta 126, 06128 Perugia, Italy. Tel: +39 0755014419 Fax: +39 0755014420 E-mail: stefania.camici@irpi.cnr.it.

22 **ABSTRACT**

23 This paper presents an innovative approach, STREAM - SaTellite based Runoff Evaluation And
24 Mapping - to derive daily river discharge and runoff estimates from satellite soil moisture,
25 precipitation and terrestrial water storage anomalies observations. Within a very simple model
26 structure, the first two variables (precipitation and soil moisture) are used to estimate the quick-flow
27 river discharge component while the terrestrial water storage anomalies are used for obtaining its
28 complementary part, i.e., the slow-flow river discharge component. The two are then summed up to
29 obtain river discharge and runoff estimates.

30 The method is tested over the Mississippi river basin for the period 2003-2016 by using Tropical
31 Rainfall Measuring Mission (TRMM) Multi-satellite Precipitation Analysis (TMPA) ~~rainfall~~
32 precipitation data, European Space Agency Climate Change Initiative (ESA CCI) soil moisture data
33 and Gravity Recovery and Climate Experiment (GRACE) terrestrial water storage data. Despite the
34 model simplicity, relatively high-performance scores are obtained in river discharge simulations, with
35 a Kling-Gupta efficiency index greater than 0.65 both at the outlet and over several inner stations
36 used for model calibration highlighting the high information content of satellite observations on
37 surface processes. Potentially useful for multiple operational and scientific applications (from flood
38 warning systems to the understanding of water cycle), the added-value of the STREAM approach is
39 twofold: 1) a simple modelling framework, potentially suitable for global runoff monitoring, at daily
40 time scale when forced with satellite observations only, 2) increased knowledge on the natural
41 processes, human activities and on their interactions on the land.

42

43 Key words: satellite products, soil moisture, water storage variations, conceptual ~~data-driven~~
44 hydrological modelling, rainfall-runoff modelling, Mississippi.

45 1. INTRODUCTION

46 Spatial and temporal continuous river discharge monitoring is paramount for improving the
47 understanding of the hydrological cycle, for planning human activities related to water use as well as
48 to prevent/mitigate the losses due to extreme flood events. To accomplish these tasks, runoff and river
49 discharge data, which represents the aggregated signal of runoff (Fekete et al., 2012), should be
50 available at adequate spatial/temporal resolution, i.e., at basin scale (basin area larger than 10'000
51 km²) and at monthly time step for water resources management and drought monitoring up to grid
52 scale (few km)/(sub-) daily time step for flood prediction. The accurate continuous (in space and
53 time) runoff and river discharge estimation at finer spatial/temporal resolution is still a big challenge
54 for hydrologists.

55 Traditional in situ observations of river discharge, even if generally characterized by high temporal
56 resolution (up to sub-hourly time step), typically offer little information on the spatial distribution of
57 runoff within a watershed. Moreover, river discharge observation networks suffer from many
58 limitations such as low station density and often incomplete temporal coverage, substantial delay in
59 data access and large decline in monitoring capacity (Vörösmarty et al. 2002). Paradoxically, this
60 latter issue is exacerbated in developing nations (Crochemore et al, 2020), where the knowledge of
61 the terrestrial water dynamics deserves greater attention due to huge damages to settlements and
62 especially the loss of human lives that occurs regularly.

63 This precarious situation has led to growing interest in finding alternative solutions, i.e., model-based
64 or observation-based approaches, for runoff and river discharge monitoring. Model-based
65 approaches, based on the mathematical description of the main hydrological processes (e.g., water
66 balance models, WBMs, global hydrological models, GHMs, e.g., Döll et al., 2003 or, increasing in
67 complexity, land surface models, LSM, e.g., Balsamo et al., 2009; Schellekens et al., 2017), are able
68 to provide comprehensive information on a large number of relevant variables of the hydrological
69 cycle including runoff and river discharge at very high temporal and spatial resolution (up to hourly

70 sampling and 0.05° grid scale). However, the values of simulated water balance components rely on
 71 a massive parameterization of the soil, vegetation and land parameters, which is not always realistic,
 72 and are strongly dependent on the GHM/ LSM models used, analysis periods (Wisser et al., 2010)
 73 and climate forcings selected (e.g Haddeland et al., 2012; Gudmundsson et al., 2012a, b; Prudhomme
 74 et al., 2014; Müller Schmied et al., 2016).
 75 Alternatively, the observation-based approaches exploit machine learning techniques and a
 76 considerable amount of data to describe the physics of the system (i.e. hydraulic and/or hydrologic
 77 phenomena, Solomatine and Ostfeld, 2008) with only a limited number of assumptions. Besides being
 78 simpler than model-based approaches, these approaches still present some limitations. At first, as they
 79 rely on a considerable amount of data describing the modelled system's physics, the spatial/temporal
 80 extent and the uncertainty of the resulting dataset is determined by the spatial/temporal coverage and
 81 the accuracy of the forcing data (e.g., see E-RUN dataset, Gudmundsson and Seneviratne, 2016;
 82 GRUN dataset, Ghiggi et al., 2019; FLO1K dataset, Barbarossa et al., 2018). Additional limitations
 83 stem from the employed method to estimate runoff. Indeed, random forests such as employed in
 84 Gudmundsson and Seneviratne, 2016, like other machine learning techniques, are powerful tools for
 85 data driven modeling, but they are prone to overfitting, implying that noise in the data can obscure
 86 possible signals (Hastie et al., 2009). Moreover, the influence of land parameters on continental-scale
 87 runoff dynamics is not taken into account as the underlying hypothesis is that the hydrological
 88 response of a basin exclusively depend on present and past atmospheric forcing. It is easy to
 89 understand that this assumption will only be valid in certain circumstances and might lead to
 90 problems, e.g., over complex terrain (Orth and Seneviratne, 2015) or in cases of human river flow
 91 regulation (Ghiggi et al., 2019).
 92 Remote sensing can provide estimates of nearly all the climate variables of the global hydrological
 93 cycle including soil moisture (e.g., Wagner et al., 2007; Seneviratne et al., 2010), precipitation
 94 (Huffman et al., 2014) and total terrestrial water storage (e.g., Houborg et al., 2012; Landerer and
 95 Swenson, 2012; Famiglietti and Rodell, 2013). It has undeniably changed and improved dramatically

96 the ability to monitor the global water cycle and, hence, runoff. By taking advantage of satellite
97 information, some studies tried to develop methodologies able to optimally produce multivariable
98 datasets from the fusion of in situ and satellite-based observations (e.g., Rodell et al., 2015; Zhang et
99 al., 2018; Pellet et al., 2019). Other studies exploited satellite observations of hydrological variables,
100 e.g., precipitation (Hong et al., 2007), soil moisture (Massari et al., 2014), and geodetic variables (e.g.,
101 Sneeuw et al., 2014; Tourian et al., 2018) to monitor single components of the water cycle in an
102 independent way.

103 Although the majority of these studies provide runoff and river discharge data at basin scale and
104 monthly time step, they deserve to be recalled here as important for the purpose of the present study.
105 In particular, Hong et al. (2007) presented a first attempt to obtain an approximate but quasi-global
106 annual streamflow dataset, by incorporating satellite precipitation data in a relatively simple rainfall-
107 runoff simulation approach. Driven by the multiyear (1998-2006) Tropical Rainfall Measuring
108 Mission Multi-satellite Precipitation Analysis, runoff was independently computed for each global
109 land surface grid cell through the Natural Resources Conservation Service (NRCS) runoff curve
110 number (CN) method (NRCS, 1986) and subsequently routed to the watershed outlet to simulate
111 streamflow. The results, compared to the in situ observed discharge data, demonstrated the potential
112 of using satellite precipitation data for diagnosing river discharge values both at global scale and for
113 medium to large river basins. If, on the one hand, the work of Hong et al. (2007) can be considered
114 as a pioneer study, on the other hand it presents a serious drawback within the NRCS-CN method
115 that lacks a realistic definition of the soil moisture conditions of the catchment before flood events.
116 This aspect is not negligible, as it is well established that soil moisture is paramount in the partitioning
117 of precipitation into surface runoff and infiltration inside a catchment (Brocca et al., 2008). In
118 particular, for the same rainfall amount but different values of initial soil moisture conditions,
119 different flooding effects can occur (see e.g. Crow et al., 2005; Brocca et al., 2008; Berthet et al.,
120 2009; Merz and Blochl, 2009; Tramblay et al., 2010). On this line following Brocca et al. (2009),
121 Massari et al. (2016) presented a very first attempt to estimate global streamflow data by using

122 satellite Soil Moisture Active and Passive (SMAP, [Entekhabi et al., 2010](#)) and Global Precipitation
123 Measurement (GPM, [Huffman et al., 2019](#)) products. Although the validation was carried out by
124 routing the monthly surface runoff only in a single basin in Central Italy, the obtained results
125 suggested to dedicate additional efforts in this direction.

126 Among the studies that use satellite observations of hydrological variables for runoff estimation, the
127 hydro-geodetic approaches are undoubtedly worth mentioning, see e.g., ([Sneeuw et al., 2014](#)) for a
128 comprehensive overview or [Lorenz et al. \(2014\)](#) for an analysis of satellite-based water balance
129 misclosures with discharge as closure term. In particular, the satellite mission Gravity Recovery And
130 Climate Experiment (GRACE), which observed the temporal changes in the gravity field, has given
131 a strong impetus to satellite-driven hydrology research ([Tapley et al., 2019](#)). Since temporal gravity
132 field variations over the continents imply water storage change, GRACE was the first remote sensing
133 system to provide observational access to deeper groundwater storage. The relation between GRACE
134 groundwater storage change and runoff was characterized by [Riegger and Tourian \(2014\)](#), which even
135 allowed the quantification of absolute drainable water storage over the Amazon ([Tourian et al., 2018](#)).
136 In essence the storage-runoff relation describes the gravity-driven drainage of a basin and, hence, the
137 slow-flow processes. Due to GRACE's spatial-temporal resolution, runoff and river discharge are
138 generally available for large basins ($>160'000 \text{ km}^2$) and at monthly time step.

139 Based on the above discussion, it is clear that each approach presents strengths and limitations that
140 enable or hamper the runoff and river discharge monitoring at finer spatial and temporal resolutions.
141 In this context, this study presents an attempt to find an alternative method to derive daily river
142 discharge and runoff estimates at $\frac{1}{4}$ degree spatial resolution exploiting satellite observations and the
143 knowledge of the key mechanisms and processes that act in the formation of runoff, i.e., the role of
144 soil moisture in determining the response of a catchment to precipitation. For that, soil moisture,
145 precipitation and terrestrial water storage anomalies (TWSA) observations are used as input into a
146 simple modelling framework named STREAM [v1.3](#) –(SaTellite based Runoff Evaluation And
147 Mapping, [version 1.3](#)). Unlike classical land surface models, STREAM exploits the knowledge of the

148 system states (i.e., soil moisture and TWSA) to derive river discharge and runoff, and thus it 1) skips
149 the modelling of the evapotranspiration fluxes which are known to be a non-negligible source of
150 uncertainty (Long et al. 2014), 2) limits the uncertainty associated with the over-parameterization of
151 soil and land parameters and 3) implicitly takes into account processes, mainly human-driven (e.g.,
152 irrigation, change in the land use), that might have a large impact on the hydrological cycle and hence
153 on runoff.

154 The detailed description of the STREAM [v1.3](#) model is given in section 4. The collected datasets and
155 the experimental design for the Mississippi River Basin (section 2) are described in sections 3 and 5,
156 respectively. Results, discussion and conclusions are drawn in section 6, 7 and 8, respectively.

157 2. STUDY AREA

158 The [STREAMSTREAM v1.3](#) model presented here has been tested and validated over the Mississippi
159 River basin. With a drainage area of about 3.3 million km², the Mississippi River basin is the fourth
160 largest watershed in the world, bordered to the West by the crest of the Rocky Mountains and to the
161 East by the crest of the Appalachian Mountains. According to the Köppen climate classification, the
162 climate is subtropical humid over the southern part of the basin, continental humid with hot summer
163 over the central part, continental humid with warm summer over the eastern and norther parts,
164 whereas a semiarid cold climate affects the western part. The average annual air temperature across
165 the watershed ranges from 4°C in the West to 6°C in the East. On average, the watershed receives
166 about 900 mm/year of precipitation (77% as rainfall and 23% as snowfall), more concentrated in the
167 eastern and southern portions of the basin with respect to its northern and western part (Vose et al.,
168 2014).

169 The river flow has a clear natural seasonality mainly controlled by spring snowmelt in the
170 mountainous areas of the basins and by heavy rainfall exceeding the soil moisture storage capacity in
171 the central and southern part of the basin (Berghuijs et al., 2016), but it is also heavily regulated by
172 the presence of about 1000 large dams (Global Reservoir and Dam Database GRanD, Lehner et al.,

2011) spread-out across the basin. The annual average of Mississippi river discharge at the Vicksburg outlet section is equal to 17'500 m³/s (see Table 1). Given the variety of climate and topography across the Mississippi River basin, it is a good candidate to test the suitability of the [STREAMSTREAM v1.3](#) model for river discharge and runoff simulation.

3. DATASETS

The datasets used in this study include in situ observations, satellite products and model outputs. The first two datasets have been used as input data to the [STREAMSTREAM v1.3](#) model. Conversely, the model outputs are used as a benchmark to validate the performance of the [STREAMSTREAM v1.3](#) model.

3.1 In situ Observations

In situ observations comprise air temperature (T_{air}) and river discharge data (Q). For T_{air} data the Climate Prediction Center (CPC) Global Temperature data developed by the American National Oceanic and Atmospheric Administration (NOAA) using the optimal interpolation of quality-controlled gauge records of the Global Telecommunication System (GTS) network (Fan et al., 2008) have been used. The dataset, downloadable at (<https://psl.noaa.gov/data/gridded/data.cpc.globaltemp.html>) is available on a global regular 0.5°×0.5° grid, and provides daily maximum (T_{max}) and minimum (T_{min}) air temperature data from 1979 to present. The daily average air temperature data have been generated as the mean of T_{max} and T_{min} of each day.

Daily Q data over the study basins have been taken from the Global Runoff Data Center (GRDC, https://www.bafg.de/GRDC/EN/Home/homepage_node.html). In particular, 11 gauging stations located along the main river network of the Mississippi River basin have been selected to represent the spatial distribution of runoff over the basin. The location of these gauging stations along with relevant characteristics (e.g., the upstream basin area, the mean annual river discharge and the presence of upstream dams) are summarized in Table 1. As it can be noted, mean annual river

198 discharge ranges from 141 to 17'500 m³/s, and 3 out 11 sections are located downstream big dams
199 ([Lehner et al., 2011](#)).

200 **3.2 Satellite Products**

201 Satellite products include observations of precipitation (*P*), soil moisture and TWSA.

202 The satellite *P* dataset used in this study is the Multi-satellite Precipitation Analysis 3B42 Version 7
203 (TMPA 3B42 V7) estimate produced by the National Aeronautics and Space Administration (NASA)
204 as the 0.25°×0.25° quasi-global (50°N-S) gridded dataset. The TMPA 3B42 V7 is a gauged-corrected
205 satellite product, with a latency period of two months after the end of the month of record, available
206 at 3h sampling interval from 1998 to present (2020). Major details about the *P* dataset, downloadable
207 from <http://pmm.nasa.gov/data-access/downloads/trmm>, can be found in [Huffman et al. \(2007\)](#).

208 Soil moisture data have been taken from the European Space Agency Climate Change Initiative (ESA
209 CCI) Soil Moisture project (<https://esa-soilmoisture-cci.org/>) that provides a [surface soil moisture](#)
210 product ([i.e., referred to first 2-3 centimeters of soil](#)) continuously updated in term of spatial-temporal
211 coverage, sensors and retrieval algorithms ([Dorigo et al., 2017](#)). In this study, the daily combined
212 ESA CCI ~~SOIL-MOISTURE~~[soil moisture](#) product v4.2 is used, that is available at global scale with
213 a grid spacing of 0.25°, for the period 1978-2016.

214 TWSA have been obtained from the Gravity Recovery And Climate Experiment (GRACE) satellite
215 mission. Here we employ the NASA Goddard Space Flight Center (GSFC) global mascon model,
216 i.e., Release v02.4, ([Luthcke et al. 2013](#)). It has been produced based on the mass concentration
217 (mascon) approach. The model provides surface mass densities on a monthly basis. Each monthly
218 solution represents the average of surface mass densities within the month, referenced at the middle
219 of the corresponding month. The model has been developed directly from GRACE level-1b K-Band
220 Ranging (KBR) data. It is computed and delivered as surface mass densities per patch over blocks of
221 approximately 1°×1° or about 12'000 km². Although the mascon size is smaller than the inherent
222 spatial resolution of GRACE, the model exhibits a relatively high spatial resolution. This is attributed

223 to a statistically optimal Wiener filtering, which uses signal and noise covariance matrices. The
224 coloured (frequency-dependent) noise characteristic of KBR data was taken in to account when
225 compiling the model, which has allowed for a reliable computation of these noise and signal
226 covariance matrices. They play a crucial role when filtering and allow to achieve a higher spatial
227 resolution compared to commonly applied GRACE filtering methods such as Gaussian smoothing
228 and/or destriping filters. GRACE data are available for the period 01 January 2003 to 15 July 2016.

229 3.3 Model Outputs

230 To establish the quality of the [STREAM v1.3](#) model in runoff simulation, monthly runoff
231 (R) data obtained from the Global Runoff Reconstruction (GRUN_v1, [https://doi.org/10.3929/ethz-](https://doi.org/10.3929/ethz-b-000324386)
232 [b-000324386](https://doi.org/10.3929/ethz-b-000324386)) have been used for comparison. The GRUN dataset ([Ghiggi et al., 2019](#)) is a global
233 monthly R dataset derived through the use of a machine learning algorithm trained with in situ Q
234 observations of relatively small catchments ($<2500 \text{ km}^2$) and gridded precipitation and temperature
235 derived from the Global Soil Wetness Project Phase 3 (GSWP3) dataset, ([Kim et al., 2017](#)). The
236 dataset covers the period from 1902 to 2014 and it is provided on a $0.5^\circ \times 0.5^\circ$ regular grid.

237 4. METHOD

238 4.1 STREAM Model: the Concept

239 The concept behind the [STREAM v1.3](#) model is that river discharge is a combination of
240 hydrological responses operating at diverse time scales ([Blöschl et al., 2013](#); [Rakovec et al., 2016](#)).
241 In particular, river discharge can be considered made up of a *slow-flow component*, produced as
242 outflow of the groundwater storage and of a *quick-flow component*, i.e. mainly related to the surface
243 and subsurface runoff components ([Hu and Li, 2018](#)).

244 While the high spatial and temporal (i.e., intermittence) variability of [rainfall-precipitation](#) and the
245 highly changing land cover spatial distribution significantly impact the variability of the *quick-flow*
246 *component* (with scales ranging from hours to days and meters to kilometres depending on the basin

size), *slow-flow river discharge* reacts to precipitation inputs more slowly (i.e., months) as water infiltrates, is stored, mixed and is eventually released in times spanning from weeks to months. Therefore, the two components can be estimated by relying upon two different approaches that involve different types of observations. Based on that, within the [STREAMSTREAM v1.3](#) model, satellite soil moisture, precipitation and TWSA will be used for deriving river discharge and runoff estimates. The first two variables are used as proxy of the *quick-flow* river discharge component while TWSA is exploited for obtaining its complementary part, i.e., the *slow-flow river discharge* component. Firstly, we exploit the role of the soil moisture in determining the response of the catchment to the precipitation inputs, which have been soundly demonstrated in more than ten years of literature studies (see e.g., [Brocca et al., 2017](#) for a comprehensive discussion on the topic). Secondly, we consider the important role of terrestrial water storage in determining the slow-flow river discharge component as modelled in several hydrological models (e.g., [Sneeuw et al., 2014](#)). It is worth noting that this *modus operandi*, i.e. to model the *quick-flow* and *slow-flow* discharge component separately exploring their process controls independently, has been largely applied and tested in recent and past studies, e.g., for the estimation of the flow duration curve (see e.g., [Botter et al., 2007a, b](#); [Yokoo and Sivapalan 2011](#); [Muneepeerakul et al., 2010](#); [Ghotbi et al., 2020](#)).

4.2 STREAM Model: the Laws

The [STREAMSTREAM v1.3](#) model is a conceptual hydrological model that, by using as input observation of P , soil moisture, TWSA and T_{air} data, simulates continuous R and Q time series. The model entails three main components (Figure 1): 1) a snow module to separate precipitation into snowfall and rainfall, 2) a soil module to simulate the evolution in time t of the quick and slow runoff responses, Q_{fu} [mm] and Q_{sl} [mm], and 3) a routing module that transfers these components through the basins and the rivers for the simulation of the *quick-flow* river discharge, QF [m³/s], and the *slow-flow* river discharge, SF [m³/s] components.

271 The soil module is composed of two storages, Su and Sl as illustrated in Figure 1. The upper storage
 272 receives inputs from P , released through a snow module ([Cislaghi et al., 2020](#)) as rainfall (r) or stored
 273 as snow water equivalent (SWE) within the snowpack and on the glaciers. In particular, according to
 274 [Cislaghi et al. \(2020\)](#), SWE is modelled by using as input T_{air} and a degree-day coefficient, C_m , to be
 275 estimated by calibration.

276 Once separated, r input contributes to the quick runoff response while the SWE (like other fluxes
 277 contributing to modify the soil water content into Su) is neglected as already considered in the satellite
 278 TWSA. Therefore, the first key point of the [STREAMSTREAM v1.3](#) model is that the water content
 279 in the upper storage is directly provided by the satellite soil moisture observations and the loss
 280 processes like infiltration or evaporation do not need to be explicitly modelled to simulate the
 281 evolution in time t of soil moisture. Consequently, the quick runoff response, Qfu from the first
 282 storage can be computed ~~through equation (1)~~ following the formulation proposed by Georgakakos
 283 and Baumer (1996), as in equation (1) ~~as follows~~:

$$284 \quad Qfu(t) = r(t) SWI(t, T)^\alpha \quad (1)$$

285 where:

286 - SWI is the Soil Water Index ([Wagner et al., 1999](#)), i.e., the root-zone soil moisture product referred
 287 to the first layer of the model ([representative of the first 5-30 centimeters of soil](#)), derived by the
 288 surface satellite soil moisture product, θ , by applying the exponential filtering approach in its
 289 recursive formulation ([Albergel et al., 2009](#)):

$$290 \quad SWI_n = SWI_{n-1} + K_n(\theta(t_n) - SWI_{n-1}) \quad (2)$$

291 with the gain K_n at the time t_n given by:

$$292 \quad K_n = \frac{K_{n-1}}{K_{n-1} + e^{\left(\frac{t_n - t_{n-1}}{T}\right)}} \quad (3)$$

293 - T [days] is a parameter, named characteristic time length, that characterizes the temporal variation
 294 of soil moisture within the root-zone profile and the gain K_n ranges between 0 and 1;

- 295 - $\alpha[-]$ is a coefficient linked to the non-linearity of the infiltration process and it takes into account
- 296 the characteristics of the soil;
- 297 - for the initialization of the filter $K_1 = 1$ and $SWI_1 = \theta(t_1)$.

298 The second key point of [STREAM v1.3 approach-model](#) concerns the estimation of the slow
 299 runoff response, Q_{sl} , from the second storage. The hypothesis here, shared also with other studies (e.g.,
 300 [Rakovec et al., 2016](#)), is that the dynamic of the slow runoff component can be represented by the
 301 monthly TWSA data. Indeed, the time scale of slow runoff response is typically in the range of seasons
 302 to years and it [can be assumed](#) ~~is~~ almost independent upon the water- that is contained in that upper
 303 storage. For that, the slow runoff response Q_{sl} , from the second storage, can be computed [following](#)
 304 [the formulation proposed by Famiglietti and Wood \(1994\)](#), through equation (4) as follows:

$$305 \quad Q_{sl}(t) = \beta (TWSA^*(t))^m \quad (4)$$

306 where:

- 307 - $TWSA^* [-]$ is the TWSA estimated by GRACE normalized by its minimum and maximum values.
- 308 The assumption behind this equation is that TWSA can be assumed as a proxy of the evolution in
 309 time, t , of the Sl , i.e., the storage of the lower storage.
- 310 - β [mm h^{-1}] and m $[-]$ are two parameters describing the nonlinearity between slow runoff
 311 component and $TWSA^*$.

312 [Note that we made the hypothesis that soil moisture and TWSA observations are independent](#)
 313 [\(whereas in the reality soil moisture can be responsible both for the generation of the quick flow part](#)
 314 [\(mainly\) and for the slow flow contribution\) given the different temporal \(and spatial\) scales at which](#)
 315 [the quick and slow runoff responses act. Note that, being based on a conceptual framework, we are](#)
 316 [assuming that soil moisture and TWSA observations are independent, whereas in the reality assume](#)
 317 [that soil moisture acts both on the generation of the quick flow part \(mainly\) and is partly responsible](#)
 318 [of the slow flow contribution indirectly via TWSA observations \(indeed TWSA already contains the](#)

~~soil moisture signal in themselves). However, this assumption can be accepted by considering the different temporal (and spatial) scales at which the quick and slow runoff responses act.~~

The [STREAMSTREAM v1.3](#) model runs in a semi-distributed version in which the catchment is divided into s elements, each one representing either a subcatchment with outlet along the main channel or an area draining directly into the main channel. Each element is assumed homogeneous and hence constitutes a lumped system.

The routing module (controlled by a γ parameter) conveys the Q_{fu} and Q_{sl} response components at each element outlet (subcatchments and directly draining areas, [Brocca et al., 2011](#)) and successively at the catchment outlet of the basin. Specifically, the quick component Q_{fu} is routed to the element outlet by the Geomorphological Instantaneous Unit Hydro-graph (GIUH, [Gupta et al., 1980](#)) for subcatchments or through a linear reservoir approach ([Nash, 1957](#)) for directly draining areas; the Q_{sl} slow component is transferred to the outlet section by a linear reservoir approach. Finally, a diffusive linear approach (controlled by the parameters C and D , i.e., Celerity and Diffusivity, [Troutman and Karlinger, 1985](#)) is applied to route the quick and slow runoff components at the outlet section of the catchment ([Brocca et al., 2011](#)). In the first case we obtain the *quick-flow* river discharge component, QF [m^3/s], and in the second case the *slow-flow* river discharge component, SF [m^3/s] (see Figure 1).

4.3 STREAM Parameters

The [STREAMSTREAM v1.3](#) model uses 8 parameters of which 5 are used in the soil module (α , T [days], β [mm h^{-1}], m , C_m) and 3 in the routing module (γ , C [km h^{-1}] and D [$\text{km}^2 \text{h}^{-1}$]). [The parameter values, –determined within the feasible parameter space \(See Table Appendix A for more details\),](#) ~~These parameters~~ are calibrated by maximizing the Kling-Gupta Efficiency index (KGE, [Gupta et al.,](#)

2009; Kling et al., 2012, see paragraph 5.1 for more details) between observed and simulated river discharge.

6.5. EXPERIMENTAL DESIGN

5.1 Modelling Setup for Mississippi River Basin

The modelling setup is carried out in four steps (Figure 2):

1. *Input data collection.* Two different groups of data have to be collected to setup the model, i.e., topographic information and hydrological variables. Concerning the topographic information, the Shuttle Elevation Derivatives at multiple Scales (HydroSHED, <https://www.hydrosheds.org/>) DEM of the basin at the 3'' resolution (nearly 90 m at the equator) as well as the location of the gauging stations where the model should be calibrated/validated, are collected. Concerning the hydrological variables, gridded precipitation, T_{air} , soil moisture and TWSA are collected. In addition, in situ Q time series for the sections where the model should be calibrated/validated as well as modelled runoff datasets are required.

2. *Sub-basin delineation.* ~~STREAM~~[STREAM v1.3](#) model is run in the semi-distributed version over the Mississippi River basin. The TopoToolbox (<https://topotoolbox.wordpress.com/>), a tool developed in Matlab by Schwanghart et al. (2010), and the DEM of the basin have been used to derive flow directions, to extract the stream network and to delineate the drainage basins over the Mississippi River basin. In particular, by considering only rivers with ~~Horton-Strahler~~ order greater than 3 ([according to the Horton-Strahler rules, Horton, 1945; Strahler, 1952](#)), the Mississippi watershed has been divided into 53 sub-basins as illustrated in Figure 3. Red dots in the figure indicate the location of the 11 discharge gauging stations selected for the study area.

[It has to be specified that the step of sub-basin delineation could be accomplished through tools different from the TopoToolbox. For instance, it could be used the free Qgis software downloadable](#)

366 at <https://www.qgis.org/it/site/forusers/download.html>, following the instruction to perform the
367 hydrological analysis as in
368 [https://docs.qgis.org/3.16/en/docs/training_manual/processing/hydro.html?highlight=hydrological%](https://docs.qgis.org/3.16/en/docs/training_manual/processing/hydro.html?highlight=hydrological%20analysis)
369 [20analysis](https://docs.qgis.org/3.16/en/docs/training_manual/processing/hydro.html?highlight=hydrological%20analysis).

370 3. *Extraction of input data.* Precipitation, T_{air} , soil moisture and TWSA datasets data have to be
371 extracted for each sub-basin of the study area. If characterized by different spatial/temporal
372 resolution, these datasets need to be resampled over a common spatial grid/temporal time step prior
373 to be used as input into the model.

374 To run the [STREAMSTREAM v1.3](#) model over the Mississippi river basin, input data have been
375 resampled over the precipitation spatial grid at 0.25° resolution through a bilinear interpolation.
376 Concerning the temporal scale, T_{air} , soil moisture and precipitation data are available at daily time
377 step, while monthly TWSA data have been linearly interpolated at daily time step. For each of the 53
378 Mississippi subbasins, the resampled precipitation, soil moisture, T_{air} and TWSA data have been
379 extracted.

380 4. *STREAM model calibration.* In situ river discharge data are used as reference data for the
381 calibration of [STREAMSTREAM v1.3](#) model. For Mississippi, the [STREAMSTREAM v1.3](#) model
382 has been calibrated over five sections as illustrated in Figure 3: the inner sections 4, 6, 9, 11 and the
383 outlet section 10, are used to calibrate the model and all sub-basins contributing to the respective
384 sections are highlighted with the same colour. This means that, for example, the sub-basins labelled
385 as 1, 2, 5 to 15, 17, 22, 23, and 30 contribute to section 4, sub-basins 31, 37, 38 and 41 contribute to
386 section 6 and so on. Consequently, the sub-basins highlighted with the same colour are assigned the
387 same model parameters, i.e. the parameters that allow to reproduce the river discharge data observed
388 at the related outlet section.

389 Once calibrated, the [STREAMSTREAM v1.3](#) model has been run to provide continuous daily Q and
390 R time series, at the outlet section of each subbasin and over each grid pixel, respectively. By
391 considering the spatial/temporal availability of both in situ and satellite observations, the entire

analysis period covers the maximum common observation period, i.e., from 01 January 2003 to 15 July 2016 at daily time scale. To establish the goodness-of-fit of the model, the simulated river discharge and runoff timeseries are compared against in situ river discharge and modelled runoff data.

5.2 Model Evaluation Criteria and Performance Metrics

The model has been run over a 13.5-year period split into two sub periods: the first 8 years, from January 2003 to December 2010, have been used to calibrate the model successively validated over the remaining 5.5 years (January 2011 - July 2016).

In particular, three different validation schemes have been adopted to assess the robustness of the [STREAMSTREAM v1.3](#) model:

1. Internal validation aimed to test the plausibility of both the model structure and the parameter set in providing reliable estimates of the hydrological variables against which the model is calibrated. For this purpose, a comparison between observed and simulated river discharge time series on the sections used for model calibration has been carried out for both the calibration and validation sub periods.
2. Cross-validation testing the goodness of the model structure and the calibrated model parameters to predict hydrological variables at locations not considered in the calibration phase. In this respect, the cross-validation has been carried out by comparing observed and simulated river discharge time series in gauged basins not considered during the calibration phase;
3. External validation aimed to test the capability of the model *“to get the right answers for the right reasons”* (Kirchner 2006). In this respect, the capability of the model to reproduce variables (e.g., fluxes or state variables) other than discharge and not considered in the calibration phase, should be tested. As runoff is a secondary product of the [STREAMSTREAM v1.3](#) model, obtained indirectly from the calibration of the river discharge (basin-integrated runoff), the comparison in terms of runoff can be considered as a further external validation of the model. Runoff, differently from discharge, cannot be directly

measured. It is generally modelled through land surface or hydrological models. Its validation requires a comparison against modelled data that, however, suffer from uncertainties (Beck et al., 2017). Based on that, in this study the GRUN runoff dataset described in the section 3.3 has been used for a qualitative comparison.

5.3 Performance Metrics

To measure the goodness-of-fit between simulated and observed river discharge data three performance scores have been used:

- the relative root mean square error, RRMSE:

$$RRMSE = \frac{\sqrt{\frac{1}{n} \sum_{i=1}^n (Q_{sim_i} - Q_{obs_i})^2}}{\frac{1}{n} \sum_{i=1}^n (Q_{obs_i})} \quad (5)$$

where Q_{obs} and Q_{sim} are the observed and simulated discharge time series of length n . RRMSE values range from 0 to $+\infty$, the lower the RRMSE, the better the agreement between observed and simulated data.

- the Pearson correlation coefficient, R , measures the linear relationship between two variables:

$$R = \frac{\sum_{i=1}^n (Q_{sim_i} - \overline{Q_{sim_i}})(Q_{obs_i} - \overline{Q_{obs_i}})}{\sqrt{\sum_{i=1}^n (Q_{sim_i} - \overline{Q_{sim_i}})^2 (Q_{obs_i} - \overline{Q_{obs_i}})^2}} \quad (6)$$

where $\overline{Q_{obs}}$ and $\overline{Q_{sim}}$ represent the mean values of Q_{obs} and Q_{sim} , respectively. The values of R range between -1 and 1 ; higher values of R indicate a better agreement between observed and simulated data.

- the Kling-Gupta efficiency index (KGE, Gupta et al., 2009), which provides direct assessment of four aspects of discharge time series, namely shape, timing, water balance and variability. It is defined as follows:

$$KGE = 1 - \sqrt{(R - 1)^2 + (\delta - 1)^2 + (\varepsilon - 1)^2} \quad (7)$$

where R is the correlation coefficient, δ the relative variability and ε the bias normalized by the standard deviation between observed and simulated discharge. The KGE values range between $-\infty$ and 1 ; the higher the KGE, the better the agreement between observed and simulated data.

442 Simulations characterized by values of KGE in the range -0.41 and 1 can be assumed as reliable;
443 values of KGE greater than 0.5 have been assumed good with respect to their ability to reproduce
444 observed time series (Thiemig et al., 2013).

445 **7.6. RESULTS**

446 The testing and validation of the [STREAM v1.3](#) model is presented and discussed in this
447 section according to the scheme illustrated in section 5.2.

448 **6.1 Internal Validation**

449 The performance of the [STREAM v1.3](#) model over the calibrated river sections is
450 illustrated in Figure 4 and summarized in Table 2. Figure 4 shows observed and simulated river
451 discharge time series over the whole study period (2003-2016); in Table 2 the performance scores are
452 evaluated separately for the calibration and validation sub periods. It is worth noting that the model
453 accurately simulates the observed river discharge data and is able to give the “right answer” with
454 good modelling performances. Score values of KGE and R over the calibration (validation) period
455 are higher than 0.62 (0.67) and 0.75 (0.75) (resp.) for all the sections; RRMSE is lower than 46%
456 (51%) for all the sections except for section 9, where it rises up to 71% (77%). The performances
457 remain good even if they are evaluated over the entire study period as indicated by the scores on the
458 top of each plot of Figure 4.

459 **6.2 Cross-validation**

460 The cross-validation has been carried out over the six river sections illustrated in Figure 5 not used
461 in the calibration step. The performance scores on the top of each plot refer to the entire study periods;
462 the scores split for calibration and validation periods are reported in Table 2. For some river sections
463 the performance is quite low (see, e.g., river section 1, 2 and 5) whereas for others the model is able
464 to simulate the observed discharge data quite accurately (e.g., 7 and 8). In particular, for river sections
465 1, 2 even if KGE reaches values equal to 0.35 and 0.40 (for the whole period), respectively, there is
466 not a good agreement between observed and simulated river discharge and the R score is lower than

0.55 for both river sections. The worst performance is obtained over section 5, with negative KGE and low R (high RRSME). These results are certainly influenced by the presence of dams located upstream to these river sections (see Table 1): the model, not having a specific module for modelling reservoirs, is not able to accurately reproduce the dynamics of river discharge over regulated river sections. Positive KGE values ~~Better performances~~ are obtained over river sections 3 ~~(slightly influenced by the presence of dams in section 1 and 2)~~, 7 and 8. In particular, over sections 3 (influenced by the presence of dams in section 1 and 2) and 7 over river section 7, (located over the Rock river, –a relatively small tributary of tributary of Mississippi river, see Table 1), the STREAMSTREAM v1.3 model overestimates the observed river discharge highlighting that the model parameters estimated for river section 4 and 6, respectively, –are not suitable to accurately reproduce river discharge for river sections 3 and 7 (see Figure 3 and Figure 5). Conversely, the performances over river section 8, whose parameters have been set equal to the ones of river section 10, are quite high (KGE equal to 0.71, 0.80 and 0.77 for the entire, the calibration and the validation period, respectively; R equal to 0.83, 0.84 and 0.84 for the entire, calibration and validation periods, respectively).

Although it is expected that the performances of STREAMSTREAM v1.3 model, as any hydrological model calibrated against observed data, can decrease over the gauging sections not used for the calibration, the findings obtained above; This finding, which could be due to different/similar interbasin characteristics, raises doubts about the robustness of model parameters and whether it is actually possible to transfer model parameters from one river section to another with different interbasin characteristics. A more in-depth investigation about the model calibration procedure and the regionalization of the model parameters will be carried out in future studies.

6.3 External Validation

For the external validation, the monthly runoff time series provided by the GRUN datasets have been compared against the ones computed by the STREAMSTREAM v1.3 model. For that, STREAMSTREAM daily runoff time series have been aggregated at monthly scale and re-gridded

493 at the same spatial resolution of the GRUN dataset (0.5°). The comparison is illustrated in Figure 6
494 for the common period 2003–2014. Although the two datasets consider different ~~rainfall~~precipitation
495 inputs, the two models agree in identifying two distinct zones in terms of runoff, i.e., the western dry
496 and the eastern wet area. This two distinct zones can be clearly identified also in the GSWP3 and
497 TMPA 3B42 V7 ~~TRMM3B42~~-precipitation maps (not shown here) used as input in GRUN and
498 STREAMSTREAM v1.3, respectively, stressing that STREAMSTREAM -runoff output is correctly
499 driven by the input data. However, ~~Likely~~—likely due to the calibration procedure, the
500 STREAMSTREAM -runoff map appears patchier with respect to GRUN and discontinuities along
501 the sub-basin boundaries (identified in Figure 3) can be noted. This should be ascribed to the
502 automatic calibration procedure of the model that, differently from other calibration techniques (e. g.,
503 regionalization procedures), does not consider the basin physical attributes like soil, vegetation, and
504 geological properties that govern spatial dynamics of hydrological processes. This calibration
505 procedure can generate sharp discontinuities even for neighbouring subcatchments individually
506 calibrated. It leads to discontinuities in model parameter values and consequently in the simulated
507 hydrological variable (runoff).

508 8.7.DISCUSSION

509 In the previous sections, the ability of the STREAMSTREAM v1.3 model to accurately simulate river
510 discharge and runoff time series has been presented. In particular, Figures 4, 5 and 6 demonstrate that
511 satellite observations of precipitation, soil moisture and terrestrial water storage anomalies can
512 provide accurate daily river discharge estimates for near-natural large basins (absence of upstream
513 dams), and for basins with draining area lower than 160'000 km² (see section 7), i.e., at
514 spatial/temporal resolution lower than the ones of the TWSA input data (monthly, 160'000 km²). This
515 is an important result of the study as it demonstrates, on one hand, that the model structure is
516 appropriate with respect to the data used as input and, on the other hand, the great value of information
517 contained into TWSA data that, even if characterized by limited spatial/temporal resolution, can be

used to simulate runoff and river discharge at basin scale. This finding has been also confirmed by a preliminary sensitivity analysis in which the STREAM v1.3 model has been run with different hydrological inputs of precipitation, soil moisture and total water storage anomaly (not shown here for brevity). In particular, by running the STREAM v1.3 model with different input configurations (e.g., by using TMPA 3B42 V7 or Climate Prediction Center (CPC) data for precipitation, ESA CCI or Advanced SCATterometer (ASCAT) data for soil moisture, TWSA or soil moisture data to simulate the slow-flow river discharge component), we found that STREAM results are more sensitive to soil moisture data rather than to precipitation input. In addition, by running STREAM v1.3 model with soil moisture data as input to simulate the slow-flow river discharge component (i.e. without using TWSA data) we found a deterioration of the model results.

Hereinafter, the strengths and the main limitations of the STREAM v1.3 approach-model are discussed.

Among the strengths of the STREAM v1.3 model it is worth highlighting:

1. **Remote sensing-based ~~data-driven~~conceptual hydrological model.** Discharge and runoff estimates are obtained through a remote sensing-based ~~data-driven~~conceptual hydrological model, simpler than classical hydrological models or LSMs. In particular, discharge and runoff estimates are obtained by exploiting as much as possible satellite observations and by keeping the modelling component at a minimum. The knowledge of the key mechanisms and processes that act in the formation of runoff, like the role of the soil moisture in determining the response of the catchment to precipitation, played a major role in the definition of the model structure. Being an observational-based approach, the STREAM v1.3 model presents two main advantages: 1) possibility to directly ingest observations (soil moisture and terrestrial water storage data) into the model structure, allowing to take implicitly into account some processes, mainly human-driven (e.g., irrigation, change in the land use), which might have a large impact on the hydrological cycle and hence on total runoff; 2) the independence with respect to existing large scale hydrological models such as, e.g., the evapotranspiration is not explicitly modelled.

544 2. **Simplicity.** The STREAM [v1.3 data-driven model](#) structure: 1) limits the input data required (only
545 precipitation, T_{air} , soil moisture and TWSA data are needed as input; LSM/GHMs require many
546 additional inputs such as wind speed, shortwave and longwave radiation, pressure and relative
547 humidity); 2) limits and simplifies the processes to be modelled for runoff/discharge simulation.
548 Processes like evapotranspiration, infiltration or percolation, are not modelled therefore avoiding the
549 need of using sophisticated and highly parameterized equations (e.g., Penman-Monteith for
550 evapotranspiration, Allen et al., 1998, Richard equation for infiltration, Richard, 1931); 3) limits the
551 number of parameters (only 8 parameters have to be calibrated) thus simplifying the calibration
552 procedure and potentially reduce the model uncertainties related to the estimation of parameter
553 values.

554 3. **Versatility.** The STREAM [v1.3](#) model is a versatile model suitable for daily runoff and discharge
555 estimation over sub-basins with different physiographic characteristics. The results obtained in this
556 study clearly indicate the potential of this approach to be extended at the global scale. Moreover, the
557 model can be easily adapted to ingest input data with spatial/temporal resolution different from the
558 one tested in this study (0.25°/daily). For instance, satellite missions with higher space/time
559 resolution, or near real time satellite products could be considered. As an example, the Next
560 Generation Gravity Mission design studies all encompass double-pair scenarios, which would greatly
561 improve upon the current spatial resolution of single-pair missions like GRACE and GRACE-FO (>
562 100'000 km²).

563 4. **Computationally inexpensive.** Due to its simplicity and the limited number of parameters to be
564 calibrated, the computational effort for the STREAM [v1.3](#) model is very limited.

565

566 However, some limitations have to be acknowledged for the current version of the STREAM [v1.3](#)
567 model:

568 1. **Presence of reservoir, diversion, dams or flood plain.** As the STREAM [v1.3](#) model does not
569 explicitly consider the presence of discontinuity elements along the river network (e. g, reservoir,

dam or floodplain), discharge estimates obtained for sections located downstream of such elements might be inaccurate (see, e.g., river sections 1 and 2 in Figure 5).

2. Need of in situ data for model calibration and robustness of model parameters. As discussed in the results section, parameter values of the STREAM [v1.3](#) model are set through an automatic calibration procedure aimed at minimizing the differences between simulated and observed river discharge. The main drawback of this parameterization technique is that the models parameterized with this technique may exhibit (1) poor predictability of state variables and fluxes at locations and periods not considered in the calibration, and (2) sharp discontinuities along sub-basin boundaries in state flux, and parameter fields (e.g., [Merz and Blöschl, 2004](#)).

To overcome these issues, several regionalization procedures, as for instance summarized in [Cislaghi et al. \(2020\)](#), could be conveniently applied to transfer model parameters from hydrologically similar catchments to a catchment of interest. In particular, the regionalization of model parameters could allow to: i) estimate discharge and runoff time series over ungauged basins overcoming the need of discharge data recorded from in-situ networks; ii) estimate the model parameter values through a physically consistent approach, linking them to the characteristics of the basins; iii) solve the problem of discontinuities in the model parameters, avoiding to obtain patchy unrealistic runoff maps. [However, this aspect is beyond the paper purpose and it will conveniently addressed in future works.](#)

9.8. CONCLUSIONS

This study presents a new [conceptual hydrological data-driven](#) model, STREAM [v1.3](#), for runoff and river discharge estimation. By using as input satellite data of precipitation, soil moisture and terrestrial water storage anomalies, the model has been able to provide accurate daily river discharge and runoff estimates at the outlet river section and the inner river sections and over a $0.25^{\circ} \times 0.25^{\circ}$ spatial grid of the Mississippi river basin. In particular, the model is suitable to reproduce:

1. river discharge time series over the calibrated river section with good performances both in calibration and validation periods;

595 2. river discharge time series over river sections not used for calibration and not located downstream
596 dams or reservoirs;

597 3. runoff time series with a quite good agreement with respect to the well-established GRUN
598 observational-based dataset used for comparison.

599 The integration of observations of soil moisture, precipitation and terrestrial water storage anomalies
600 is a first alternative method for river discharge and runoff estimation with respect to classical methods
601 based on the use of TWSA-only (suitable for river basins larger than 160'000 km², monthly time
602 scale) or on classical LSMs (Cai et al., 2014).

603 Moreover, although simple, the model has demonstrated a great potential to be easily applied over
604 subbasins with different climatic and topographic characteristics, suggesting also the possibility to
605 extend its application to other basins. In particular, the analysis over basins with high human impact,
606 where the knowledge of the hydrological cycle and the river discharge monitoring is very important,
607 deserves special attention. Indeed, as the STREAM [v1.3](#) model is directly ingesting observations of
608 soil moisture and terrestrial water storage data, it allows the modeller to neglect processes that are
609 implicitly accounted for in the input data. Therefore, human-driven processes (e.g., irrigation, land
610 use change), that are typically very difficult to simulate due to missing information and might have a
611 large impact on the hydrological cycle, hence on total runoff, could be implicitly modelled. The
612 application of the STREAM [v1.3](#) model on a larger number of basins [with different climatic-](#)
613 [physiographic characteristics \(e.g., including more arid basins, snow-dominated, lots of topography,](#)
614 [heavily managed\) will be object of future studies and it will allow](#) ~~is also required to~~ ~~to~~ investigate
615 the possibility to regionalize the model parameters and overcome the limitations of the automatic
616 calibration procedure highlighted in the discussion section.

617 **AUTHOR CONTRIBUTION**

618 S.C. performed the analysis and wrote the manuscript. G.G. collected the data and helped in
619 performing the analysis; C.M, L.B., A.T., N.S., H.H.F., C.M., M.R. and J.B. contributed to the
620 supervision of the work. All authors discussed the results and contributed to the final manuscript.

621 **CODE AVAILABILITY**

622 [The STREAM model version 1.3, with a short user manual, –is freely downloadable in Zenodo](https://zenodo.org/record/4744984#.YJj4MLUzaUk)
623 [\(https://zenodo.org/record/4744984#.YJj4MLUzaUk, doi: 10.5281/zenodo.4744984\). The STREAM](https://zenodo.org/record/4744984#.YJj4MLUzaUk)
624 [v1.3 model code is distributed through M language files, but it could be run with different interpreters](https://zenodo.org/record/4744984#.YJj4MLUzaUk)
625 [of M language, like the GNU Octave \(freely downloadable here](https://zenodo.org/record/4744984#.YJj4MLUzaUk)
626 [https://www.gnu.org/software/octave/download\). The STREAM model code will be made available](https://zenodo.org/record/4744984#.YJj4MLUzaUk)
627 ~~[once the manuscript will be published.](https://zenodo.org/record/4744984#.YJj4MLUzaUk)~~

628 **DATA AVAILABILITY**

629 All data and codes used in the study are freely available online. Air temperature data are available at
630 <https://psl.noaa.gov/data/gridded/data.cpc.globaltemp.html> (last access 25/11/202). In situ river
631 discharge data have been taken from the Global Runoff Data Center (GRDC,
632 https://www.bafg.de/GRDC/EN/Home/homepage_node.html (last access 25/11/202). Precipitation
633 and soil moisture data are available from <http://pmm.nasa.gov/data-access/downloads/trmm> and
634 <https://esa-soilmoisture-cci.org/>, respectively.

635 **COMPETING INTERESTS**

636 The authors declare that they have no conflict of interest.

637 **ACKNOWLEDGMENTS**

638 The authors wish to thank the Global Runoff Data Centre (GRDC) for providing most of the
639 streamflow data throughout Europe. The authors gratefully acknowledge support from ESA through
640 the STREAM Project (EO Science for Society element Permanent Open Call contract n°
641 4000126745/19/I-NB).

642

643 REFERENCE

- 644 Albergel, C., Rüdiger, C., Carrer, D., Calvet, J. C., Fritz, N., Naeimi, V., Bartalis, Z., & Hasenauer, S. (2009). An
645 evaluation of ASCAT surface soil moisture products with in-situ observations in southwestern France. *Hydrology and*
646 *Earth System Sciences*, 13, 115–124, doi:10.5194/hess-13-115-2009.
- 647 Allen RG, Pereira LS, Raes D, Smith M (1998) Crop evapotranspiration — guidelines for computing crop water
648 requirements. FAO Irrigation & Drainage Paper 56. FAO, Rome.
- 649 Balsamo, G., A. Beljaars, K. Scipal, P. Viterbo, B. vanden Hurk, M. Hirschi, and A. K. Betts (2009). A revised hydrology
650 for the ECMWF model: Verification from field site to terrestrial water storage and impact in the integrated forecast
651 system, *J. Hydrometeorol.*, 10(3), 623–643, doi:10.1175/2008JHM1068.1.
- 652 Barbarossa, V., Huijbregts, M. A., Beusen, A. H., Beck, H. E., King, H., & Schipper, A. M. (2018). FLO1K, global maps
653 of mean, maximum and minimum annual streamflow at 1 km resolution from 1960 through 2015. *Scientific data*, 5,
654 180052.
- 655 Beck, H. E., van Dijk, A. I., de Roo, A., Dutra, E., Fink, G., Orth, R., & Schellekens, J. (2017). Global evaluation of
656 runoff from ten state-of-the-art hydrological models. *Hydrology and Earth System Sciences*, 21(6), 2881-2903. doi;
657 doi.org/10.5194/hess-21-2881-2017.
- 658 Berghuijs, W. R., Woods, R. A., Hutton, C. J., and Sivapalan, M. (2016). Dominant flood generating mechanisms across
659 the United States, *Geophys. Res. Lett.*, 43, 4382–4390, <https://doi.org/10.1002/2016GL068070>.
- 660 Berthet, L., Andréassian, V., Perrin, C., & Javelle, P. (2009). How crucial is it to account for the antecedent moisture
661 conditions in flood forecasting? Comparison of event-based and continuous approaches on 178 catchments.
662 *Hydrology and Earth System Sciences*, 13(6), 819-831.
- 663 Blöschl, G., Sivapalan, M., Wagener, T., Viglione, A., & Savenije, H. H. G. (Eds.) (2013). *Runoff predictions in ungauged*
664 *basins: A synthesis across processes, places and scales*. Cambridge: Cambridge University Press.
- 665 Botter, G., Peratoner, F., Porporato, A., Rodriguez-Iturbe, I., and Rinaldo, A. (2007b). Signatures of large-scale soil
666 moisture dynamics on streamflow statistics across U.S. Climate regimes, *Water Resour. Res.*, 43, W11413,
667 doi:10.1029/2007WR006162.
- 668 Botter, G., Porporato, A., Daly, E., Rodriguez-Iturbe, I., and Rinaldo, A. (2007a). Probabilistic characterization of base
669 flows in river basins: Roles of soil, vegetation, and geomorphology, *Water Resour. Res.*, 43,
670 W06404, doi:10.1029/2006WR005397.
- 671 Brocca, L., Melone, F., Moramarco, T. (2008). On the estimation of antecedent wetness conditions in rainfall-runoff
672 modelling. *Hydrological Processes*, 22 (5), 629-642, doi:10.1002/hyp.6629. <http://dx.doi.org/10.1002/hyp.6629>.
- 673 Brocca, L., Melone, F., Moramarco, T., & Morbidelli, R. (2009). Antecedent wetness conditions based on ERS
674 scatterometer data. *Journal of Hydrology*, 364(1-2), 73-87
- 675 Brocca, L., Melone, F., & Moramarco, T. (2011). Distributed rainfall-runoff modelling for flood frequency estimation
676 and flood forecasting. *Hydrological processes*, 25(18), 2801-2813.
- 677 Brocca, L., Ciabatta, L., Massari, C., Camici, S., & Tarpanelli, A. (2017). Soil moisture for hydrological applications:
678 open questions and new opportunities. *Water*, 9(2), 140.
- 679 Cai, X., Yang, Z. L., David, C. H., Niu, G. Y., & Rodell, M. (2014). Hydrological evaluation of the Noah-MP land surface
680 model for the Mississippi River Basin. *Journal of Geophysical Research: Atmospheres*, 119(1), 23-38.
- 681 Cislighi, A., Masseroni, D., Massari, C., Camici, S., & Brocca, L. (2020). Combining a rainfall–runoff model and a
682 regionalization approach for flood and water resource assessment in the western Po Valley, Italy. *Hydrological*
683 *Sciences Journal*, 65(3), 348-370.
- 684 Crochemore, L., Isberg, K., Pimentel, R., Pineda, L., Hasan, A., & Arheimer, B. (2020). Lessons learnt from checking
685 the quality of openly accessible river flow data worldwide. *Hydrological Sciences Journal*, 65(5), 699-711
- 686 Crow, W. T., Bindlish, R., & Jackson, T. J. (2005). The added value of spaceborne passive microwave soil moisture
687 retrievals for forecasting rainfall-runoff partitioning. *Geophysical Research Letters*, 32(18).

688 Döll, P., F.Kaspar, and B.Lehner (2003), A global hydrological model for deriving water availability indicators: Model
689 tuning and validation, *J. Hydrol.*, 270(1–2), 105–134, doi:10.1016/S0022-1694(02)00283-4.

690 Dorigo, W., Wagner, W., Albergel, C., Albrecht, F., Balsamo, G., Brocca, L., Chung, D., Ertl, M., Forkel, M., Gruber, A.,
691 Haas, D., Hamer, P. Hirschi, M., Ikonen, J., de Jeu, R., Kidd, R., Lahoz, W., Liu, Y.Y., Miralles, D., Mistelbauer, T.,
692 Nicolai-Shaw, N., Parinussa, R., Pratola, C., Reimer, C., van der Schalie, R., Seneviratne, S.I., Smolander, T.,
693 Lecomte, P. (2017). ESA CCI Soil Moisture for improved Earth system understanding: state-of-the art and future
694 directions. *Remote Sensing of Environment*, 203, 185–215.

695 [Entekhabi, D., Njoku, E. G., O'Neill, P. E., Kellogg, K. H., Crow, W. T., Edelstein, W. N., ... & Van Zyl, J. \(2010\). The](#)
696 [soil moisture active passive \(SMAP\) mission. *Proceedings of the IEEE*, 98\(5\), 704-716. doi:](#)
697 [10.1109/JPROC.2010.2043918.](#)

698 [Famiglietti, J.S., Wood, E. F. \(1994\). Multiscale modeling of spatially variable water and energy balance processes. *Water*](#)
699 [Resour. Res.](#), 30, 3061–3078.

700 Famiglietti, J. S., & Rodell, M. (2013). Water in the balance. *Science*, 340(6138), 1300–1301.

701 Fan, Y. & Van den Dool, H. A (2008). Global monthly land surface air temperature analysis for 1948–present. *Journal of*
702 *Geophysical Research: Atmospheres* 113, D01103.

703 Fekete, B. M., Looser, U., Pietroniro, A., and Robarts, R. D. (2012). Rationale for monitoring discharge on the ground,
704 *J. Hydrometeorol.*, 13, 1977–1986.

705 [Georgakakos KP, Baumer OW. \(1996\). Measurement and utilization of onsite soil moisture data. *Journal of Hydrology*](#)
706 [184: 131–152.](#)

707 Ghiggi, G., Humphrey, V., Seneviratne, S. I., & Gudmundsson, L. (2019). GRUN: an observation-based global gridded
708 runoff dataset from 1902 to 2014. *Earth System Science Data*, 11(4), 1655–1674.

709 Ghotbi, S., Wang, D., Singh, A., Blöschl, G., & Sivapalan, M. (2020). A New Framework for Exploring Process Controls
710 of Flow Duration Curves. *Water Resources Research*, 56(1), e2019WR026083.

711 Gudmundsson, L., & Seneviratne, S. I. (2016). Observation-based gridded runoff estimates for Europe (E-RUN version
712 1.1). *Earth System Science Data*, 8(2), 279–295.

713 Gudmundsson, L., Wagener, T., Tallaksen, L. M., & Engeland, K. (2012a). Evaluation of nine large-scale hydrological
714 models with respect to the seasonal runoff climatology in Europe. *Water Resources Research*, 48(11).

715 Gudmundsson, L., Tallaksen, L. M., Stahl, K., Clark, D. B., Du-mont, E., Hagemann, S., Bertrand, N., Gerten, D., Heinke,
716 J., Hanasaki, N., Voss, F., and Koirala, S. (2012b). Comparing Large-Scale Hydrological Model Simulations to
717 Observed Runoff Percentiles in Europe, *J. Hydrometeorol.*, 13, 604–62.

718 Gupta VK, Waymire E, Wang CT. (1980). A representation of an instantaneous unit hydrograph from geomorphology.
719 *Water Resources Research* 16: 855–862, doi: 10.1029/WR016i005p00855.

720 Gupta, H. V., Kling, H., Yilmaz, K. K., & Martinez, G. F. (2009). Decomposition of the mean squared error and NSE
721 performance criteria: Implications for improving hydrological modelling. *Journal of Hydrology*, 377(1–2), 80–91.

722 Haddeland, I., Heinke, J., Voß, F., Eisner, S., Chen, C., Hagemann, S., & Ludwig, F. (2012). Effects of climate model
723 radiation, humidity and wind estimates on hydrological simulations. *Hydrology and Earth System Sciences*, 16(2),
724 305–318.

725 Hastie, T., Tibshirani, R., and Friedman, J. H. (2009). *The Elements of Statistical Learning – Data Mining, Inference, and*
726 *Prediction*, Second Edition, Springer Series in Statistics, Springer, New York, 2nd Edn., available at: [http://www-](http://www-stat.stanford.edu/~tibs/ElemStatLearn/)
727 [stat.stanford.edu/~tibs/ElemStatLearn/](http://www-stat.stanford.edu/~tibs/ElemStatLearn/) (last access: 5 July 2016).

728 Hong, Y., Adler, R. F., Hossain, F., Curtis, S., & Huffman, G. J. (2007). A first approach to global runoff simulation
729 using satellite rainfall estimation. *Water Resources Research*, 43(8).

730 [Horton, R. E. \(1945\). Hydrological approach to quantitative morphology. *Geol. Soc. Am. Bull.*, 56, 275-370.](#)

731 Houborg, R., Rodell, M., Li, B., Reichle, R., & Zaitchik, B. F. (2012). Drought indicators based on model-assimilated
732 Gravity Recovery and Climate Experiment (GRACE) terrestrial water storage observations. *Water Resources*
733 *Research*, 48(7).

734 Hu GR., Li XY. (2018). Subsurface Flow. In: Li X., Vereecken H. (eds) Observation and Measurement. Ecohydrology.
735 Springer, Berlin, Heidelberg. https://doi.org/10.1007/978-3-662-47871-4_9-1

736 Huffman, G. J., R. F. Adler, D. T. Bolvin, G. J. Gu, E. J. Nelkin, K. P. Bowman, Y. Hong, E. F. Stocker, and D. B. Wolff.
737 (2007). The TRMM Multisatellite Precipitation Analysis (TMPA): Quasi-Global, Multiyear, Combined-Sensor
738 Precipitation Estimates at Fine Scales. *Journal of Hydrometeorology* 8 (1): 38–55. doi:10.1175/jhm560.1.

739 Huffman, G. J., Stocker, E. F., Bolvin, D. T., Nelkin, E. J., & Adler, R. F. (2014). TRMM Version 7 3B42 and 3B43 Data
740 Sets. NASA/GSFC, Greenbelt, MD.

741 [Huffman, G. J., Bolvin, D. T., Braithwaite D., Hsu K., Joyce R., Kidd C., Nelkin Eric J., Sorooshian S., Tan J., Xie P.](https://docserver.gesdisc.eosdis.nasa.gov/public/project/GPM/IMERG_ATBD_V06.pdf)
742 [\(2019\). NASA Global Precipitation Measurement \(GPM\) Integrated Multi-satellite Retrievals for GPM \(IMERG\).](https://docserver.gesdisc.eosdis.nasa.gov/public/project/GPM/IMERG_ATBD_V06.pdf)
743 [https://docserver.gesdisc.eosdis.nasa.gov/public/project/GPM/IMERG_ATBD_V06.pdf.](https://docserver.gesdisc.eosdis.nasa.gov/public/project/GPM/IMERG_ATBD_V06.pdf)

744 Kim, H., Watanabe, S., Chang, E. C., Yoshimura, K., Hirabayashi, J., Famiglietti, J., and Oki, T. (2017). Global Soil
745 Wetness Project Phase 3 Atmospheric Boundary Conditions (Experiment 1) [Data set], Data Integration and Analysis
746 System (DIAS), <https://doi.org/10.20783/DIAS.501>.

747 Kirchner, J. W. (2006). Getting the right answers for the right reasons: Linking measurements, analyses, and models to
748 advance the science of hydrology. *Water Resources Research*, 42(3).

749 Kling, H., Fuchs, M., & Paulin, M. (2012). Runoff conditions in the upper Danube basin under an ensemble of climate
750 change scenarios. *Journal of Hydrology*, 424, 264–277, doi: 10.1016/j.jhydrol.2012.01.011.

751 Landerer, F. W., & Swenson, S. C. (2012). Accuracy of scaled GRACE terrestrial water storage estimates. *Water*
752 *resources research*, 48(4).

753 Lehner, B., C. Reidy Liermann, C. Revenga, C. Vörösmarty, B. Fekete, P. Crouzet, P. Döll, M. Endejan, K. Frenken, J.
754 Magome, C. Nilsson, J.C. Robertson, R. Rodel, N. Sindorf, and D. Wisser. 2011. High-resolution mapping of the
755 world's reservoirs and dams for sustainable river-flow management. *Frontiers in Ecology and the Environment* 9 (9):
756 494–502.

757 Long, D., Longuevergne, L., & Scanlon, B. R. (2014). Uncertainty in evapotranspiration from land surface modeling,
758 remote sensing, and GRACE satellites. *Water Resources Research*, 50(2), 1131–1151.

759 Lorenz, C., H. Kunstmann, B. Devaraju, M. J. Tourian, N. Sneeuw, and J. Riegger (2014). Large-Scale Runoff from
760 Landmasses: A Global Assessment of the Closure of the Hydrological and Atmospheric Water Balances. *J.*
761 *Hydrometeor.*, 15, 2111–2139, doi:10.1175/JHM-D-13-0157.1.

762 Luthcke, S.B., Sabaka, T.J., Loomis, B.D., Arendt, A.A., McCarthy, J.J., Camp, J. (2013) Antarctica, Greenland and Gulf
763 of Alaska land-ice evolution from an iterated GRACE global mascon solution, *Journal of Glaciology*, Vol. 59, No.
764 216, 2013 doi:10.3189/2013JoG12J147.

765 Massari, C., Brocca, L., Tarpanelli, A., Hong, Y., Crow, W., Ciabatta, L., Camici, S., Barbetta, S., Moramarco, T. (2016).
766 Global surface runoff estimation in near real time by using SMAP and GPM, poster at SMAP conference.

767 Massari, C., Brocca, L., Barbetta, S., Papathanasiou, C., Mimikou, M., & Moramarco, T. (2014). Using globally available
768 soil moisture indicators for flood modelling in Mediterranean catchments. *Hydrology and Earth System Sciences*,
769 18(2), 839.

770 Merz, R., & Blöschl, G. (2009). A regional analysis of event runoff coefficients with respect to climate and catchment
771 characteristics in Austria. *Water Resources Research*, 45(1).

772 Mueller Schmied, H., Adam, L., Eisner, S., Fink, G., Flörke, M., Kim, H., ... & Song, Q. (2016). Variations of global and
773 continental water balance components as impacted by climate forcing uncertainty and human water use. *Hydrology*
774 *and Earth System Sciences*, 20(7), 2877–2898.

775 Muneeppeerakul, R., Azale, S., Botter, G., Rinaldo, A., & Rodriguez-Iturbe, I. (2010). Daily streamflow analysis based
776 on a two-scaled gamma pulse model. *Water Resources Research*, 46(11).

777 Nash, J. E. (1957). The form of the instantaneous unit hydrograph, IASH publication no. 45, 3–4, 114–121.

778 Natural Resources Conservation Service (NRCS) (1986), Urban hydrology for small watersheds, Tech. Release 55, 2nd
779 ed., U.S. Dep. of Agric., Washington, D. C. (available at [ftp://ftp.wcc.nrcs.usda.gov/downloads/](ftp://ftp.wcc.nrcs.usda.gov/downloads/hydrology_hydraulics/tr55/tr55.pdf)
780 [hydrology_hydraulics/tr55/tr55.pdf](ftp://ftp.wcc.nrcs.usda.gov/downloads/hydrology_hydraulics/tr55/tr55.pdf))

Orth, R., & Seneviratne, S. I. (2015). Introduction of a simple-model-based land surface dataset for Europe. *Environmental Research Letters*, 10(4), 044012.

Pellet, V., Aires, F., Munier, S., Fernández Prieto, D., Jordá, G., Dorigo, W. A., ... & Brocca, L. (2019). Integrating multiple satellite observations into a coherent dataset to monitor the full water cycle—application to the Mediterranean region. *Hydrology and Earth System Sciences*, 23(1), 465-491.

Prudhomme, C., Giuntoli, I., Robinson, E. L., Clark, D. B., Arnell, N. W., Dankers, R., ... & Hagemann, S. (2014). Hydrological droughts in the 21st century, hotspots and uncertainties from a global multimodel ensemble experiment. *Proceedings of the National Academy of Sciences*, 111(9), 3262-3267.

Rakovec, O., Kumar, R., Attinger, S., & Samaniego, L. (2016). Improving the realism of hydrologic model functioning through multivariate parameter estimation. *Water Resources Research*, 52(10), 7779-7792.

Richards, L.A. (1931). Capillary conduction of liquids through porous mediums. *Physics*. 1 (5): 318–333. Bibcode:1931Physi.1.318R. doi:10.1063/1.1745010.

Riegger, J., and M. J. Tourian (2014), Characterization of runoff-storage relationships by satellite gravimetry and remote sensing, *Water Resour. Res.*, 50, 3444–3466, doi:10.1002/2013WR013847.

Rodell, M., Beaudoin, H. K., L’Ecuyer, T. S., Olson, W. S., Famiglietti, J. S., Houser, P. R., Adler, R., Bosilovich, M. G., Clayson, C. A., Chambers, D., Clark, E., Fetzer, E. J., Gao, X., Gu, G., Hilburn, K., Huffman, G. J., Lettenmaier, D. P., Liu, W. T., Robertson, F. R., Schlosser, C. A., Sheffield, J. and Wood, E. F. (2015). The observed state of the water cycle in the early 15twenty-first century, *J. Clim.*, 28(21), 8289–8318, doi:10.1175/JCLI-D-14-00555.1.

Schellekens, J., Dutra, E., Martínez-de la Torre, A., Balsamo, G., van Dijk, A., Sperna Weiland, F., Minvielle, M., Calvet, J.-C., Decharme, B., Eisner, S., Fink, G., Flörke, M., Peßenteiner, S., van Beek, R., Polcher, J., Beck, H., Orth, R., Calton, B., Burke, S., Dorigo, W., and Weedon, G. P. (2017). A global water resources ensemble of hydrological models: the earth2Observe Tier-1 dataset, *Earth Syst. Sci. Data*, 9, 389–413, <https://doi.org/10.5194/essd-9-389-2017>.

Schwanghart, W., & Kuhn, N. J. (2010). TopoToolbox: A set of Matlab functions for topographic analysis. *Environmental Modelling & Software*, 25(6), 770-781.

Seneviratne, S. I., Corti, T., Davin, E. L., Hirschi, M., Jaeger, E. B., Lehner, I., ... & Teuling, A. J. (2010). Investigating soil moisture–climate interactions in a changing climate: A review. *Earth-Science Reviews*, 99(3-4), 125-161.

Sneeuw, N., Lorenz, C., Devaraju, B., Tourian, M. J., Riegger, J., Kunstmann, H., & Bárdossy, A. (2014). Estimating runoff using hydro-geodetic approaches. *Surveys in Geophysics*, 35(6), 1333-1359.

Solomatine, D. P., & Ostfeld, A. (2008). Data-driven modelling: some past experiences and new approaches. *Journal of hydroinformatics*, 10(1), 3-22.

[Strahler, A. N. \(1952\). Hypsometric \(area-altitude\) analysis of erosional topography. *Geological Society of America Bulletin*, 63\(11\), 1117-1142.](#)

Tapley, B.D., Watkins, M.M., Flechtner, F. et al. (2019). Contributions of GRACE to understanding climate change. *Nat. Clim. Chang.* 9, 358–369, doi:10.1038/s41558-019-0456-2.

Thiemig, V., Rojas, R., Zambrano-Bigiarini, M., & De Roo, A. (2013). Hydrological evaluation of satellite rainfall estimates over the Volta and Baro-Akobo Basin. *Journal of Hydrology*, 499, 324-338.

Tourian, M. J., Reager, J. T., & Sneeuw, N. (2018). The total drainable water storage of the Amazon river basin: A first estimate using GRACE. *Water Resources Research*, 54. <https://doi.org/10.1029/2017WR021674>.

Tramblay, Y., Bouvier, C., Martin, C., Didon-Lescot, J. F., Todorovik, D., & Domergue, J. M. (2010). Assessment of initial soil moisture conditions for event-based rainfall–runoff modelling. *Journal of Hydrology*, 387(3-4), 176-187.

Troutman, B. M., Karlinger, M.B. (1985). Unit hydrograph approximation assuming linear flow through topologically random channel networks. *Water Resources Research*, 21: 743 – 754, doi: 10.1029/WR021i005p00743.

Vose, R.S., Applequist, S., Durre, I., Menne, M.J., Williams, C.N., Fenimore, C., Gleason, K., & Arndt, D. (2014). Improved Historical Temperature and Precipitation Time Series For U.S. Climate Divisions. *Journal of Applied Meteorology and Climatology*, 53(May), 1232–1251. DOI: 10.1175/JAMC-D-13-0248.1

Vörösmarty C. J., and Coauthors (2002). Global water data: A newly endangered species. *Eos, Trans. Amer. Geophys. Union*, 82, 54.

828 Wagner, W., Blöschl, G., Pampaloni, P., Calvet, J. C., Bizzarri, B., Wigneron, J. P., & Kerr, Y. (2007). Operational
829 readiness of microwave remote sensing of soil moisture for hydrologic applications. *Hydrology Research*, 38(1), 1-
830 20.

831 Wagner, W., Lemoine, G., & Rott, H. (1999). A method for estimating soil moisture from ERS scatterometer and soil
832 data. *Remote Sensing of Environment*, 70, 191–207, doi:10.1016/S0034-4257(99)00036-X.

833 Wisser, D., Fekete, B. M., Vörösmarty, C. J., and Schumann, A. H. (2010). Reconstructing 20th century global
834 hydrography: a contribution to the Global Terrestrial Network- Hydrology (GTN-H), *Hydrol.Earth Syst. Sci.*, 14, 1–
835 24, doi:10.5194/hess-14-1-2010.

836 Yokoo, Y., & Sivapalan, M. (2011). Towards reconstruction of the flow duration curve: Development of a conceptual
837 framework with a physical basis. *Hydrology and Earth System Sciences*, 15(9), 2805–2819.
838 <https://doi.org/10.5194/hess-15-2805-2011>.

839 Zhang, Y., Pan, M., Sheffield, J., Siemann, A. L., Fisher, C. K., Liang, M., ... & Zhou, T. (2018). A Climate Data Record
840 (CDR) for the global terrestrial water budget: 1984–2010. *Hydrology and Earth System Sciences (Online)*, 22(PNNL-
841 SA-129750).

842

843 Table 1. Location of gauging stations over the Mississippi basins and upstream contributing area.
844 Bold text Red-colored is used to text indicates stations where the STREAM [v1.3](#) model has been
845 calibrated.

#	River	Station name	Latitude (°)	Longitude (°)	Upstream area (km ²)	Mean annual river discharge (m ³ /s)	Presence of dam
1	Missouri	Bismarck, ND	-100.82	46.81	481'232	633	Garrison dam
2	Missouri	Omaha, NE	-95.92	41.26	814'371	914	Gavins Point Dam
3	Missouri	Kansas City, MO	-94.59	39.11	1'229'427	1499	---
4	Missouri	Hermann, MO	-91.44	38.71	1'330'000	2326	---
5	Kansas	Wamego, KS	-96.30	39.20	143'054	141	Kanopolis
6	Mississippi	Keokuk, IA	-91.37	40.39	282'559	1948	---
7	Rock	Near Joslin, IL	-90.18	41.56	23'835	199	---
8	Mississippi	Chester, IL	-89.84	37.90	1'776'221	6018	---
9	Arkansas	Murray Dam Near Little Rock, AR	-92.36	34.79	408'068	1249	---
10	Mississippi	Vicksburg, MS	-90.91	32.32	2'866'590	17487	---
11	Ohio	Metropolis, ILL.	-88.74	37.15	496'134	7931	---

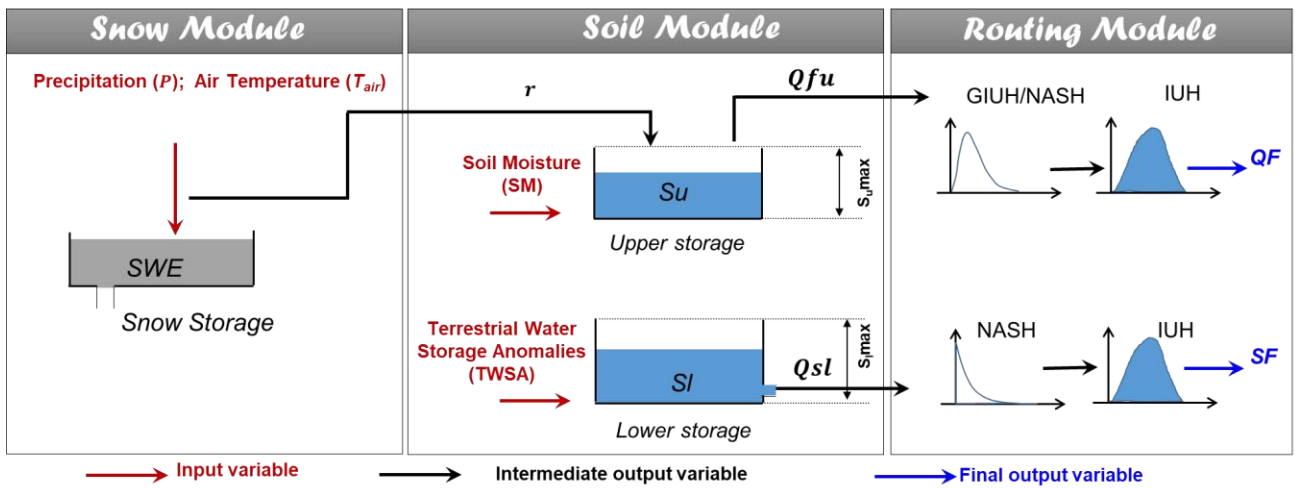
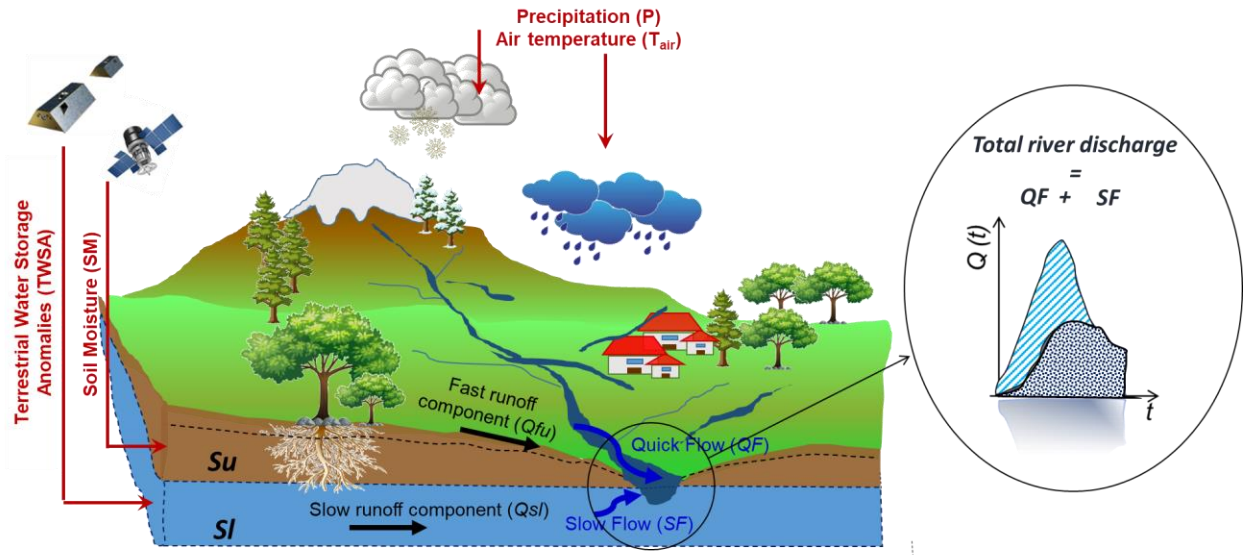
846
847

848 Table 2. Performance scores obtained over the Mississippi river sections during the calibration and
849 validation periods.

#	CALIBRATION PERIOD			VALIDATION PERIOD		
SCORE	KGE (-)	R (-)	RRMSE (%)	KGE (-)	R (-)	RRMSE (%)
CALIBRATED SECTIONS						
10	0.78	0.78	30	0.74	0.80	38
9	0.62	0.75	71	0.67	0.85	77
6	0.83	0.84	39	0.73	0.84	46
4	0.77	0.78	46	0.72	0.75	50
11	0.82	0.82	44	0.70	0.86	51
SECTIONS NOT USED FOR CALIBRATION						
1	-3.26	0.08	137	0.20	0.44	96
2	-0.57	0.48	118	0.40	0.53	89
3	0.16	0.71	83	0.39	0.70	72
5	-1.49	0.24	368	-1.26	0.31	358
7	0.53	0.68	71	0.20	0.70	81
8	0.80	0.84	36	0.77	0.84	39

850

851

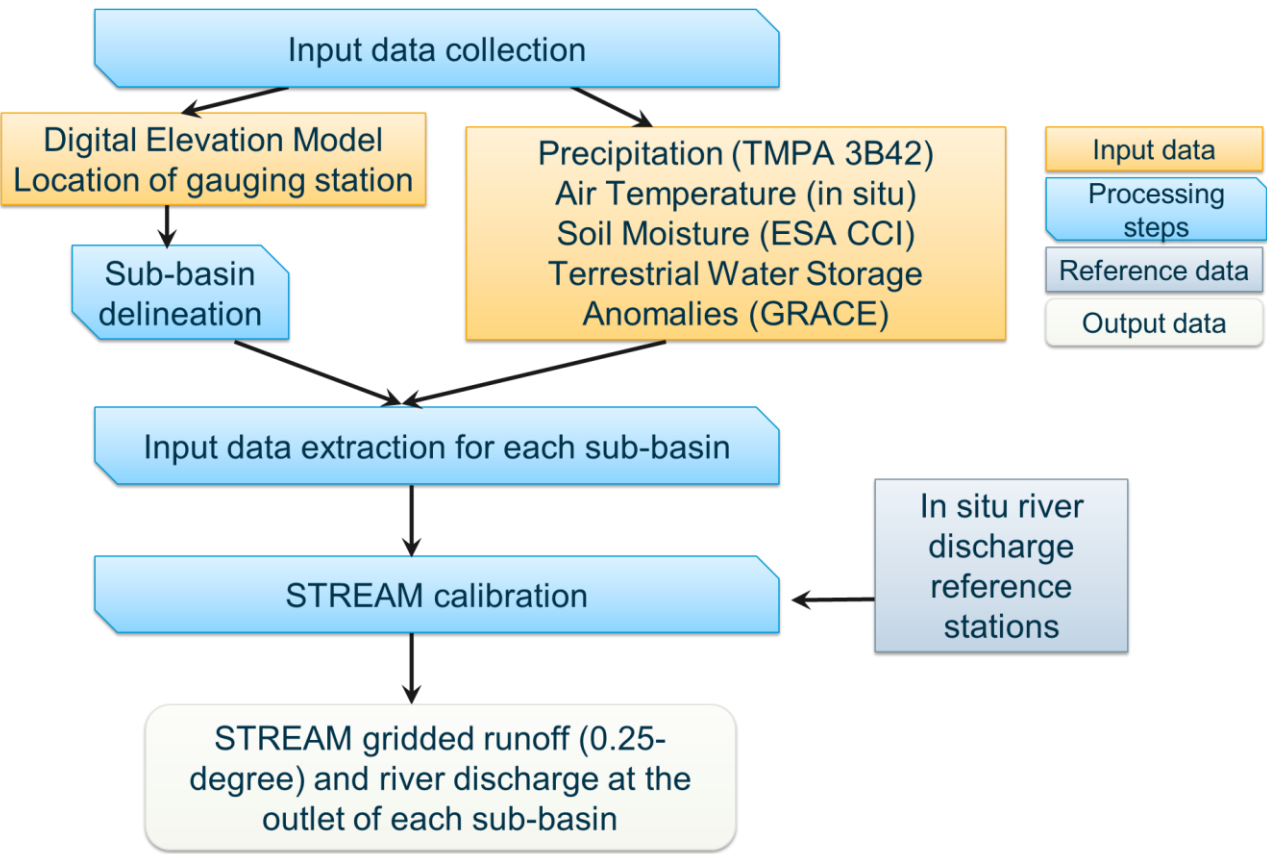


852

853 Figure 1. Configuration of the STREAM [v1.3](#) model adopted for total runoff estimation. The model
 854 includes three modules, the snow module allowing to separate snowfall from [rainfall precipitation](#), the
 855 soil module that simulates the slow and quick runoff components (Q_{su} and Q_{fu} , respectively) and the
 856 routing module for flood simulation. Red arrows indicate input variables; black arrows indicate
 857 intermediate output variables; blue arrows indicate final output variables. The components Q_{fu} and
 858 Q_{su} are computed by using satellite P , soil moisture and TWSA data as input to the soil module.
 859 Please refer to text for symbols.

860

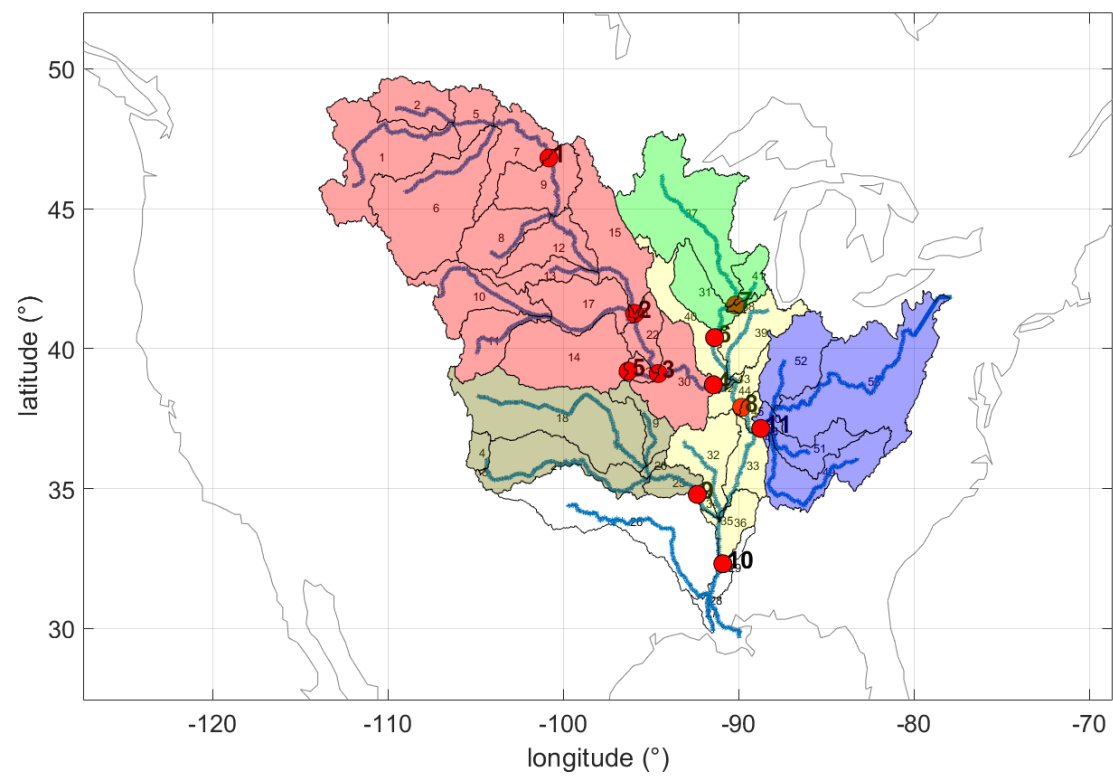
861



862
863
864
865

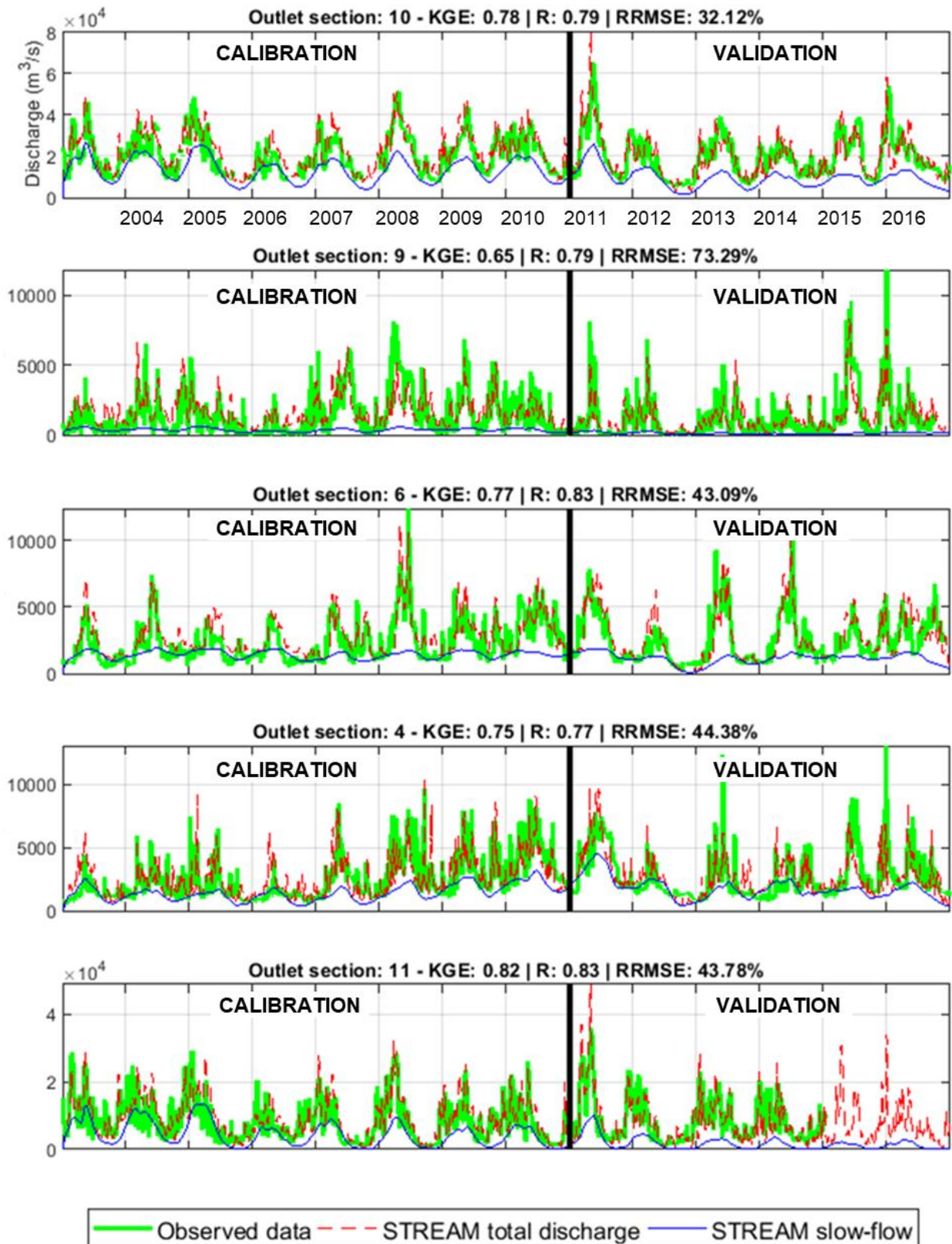
Figure 2. Processing steps of the STREAM [v1.3 approach model](#).

866



867

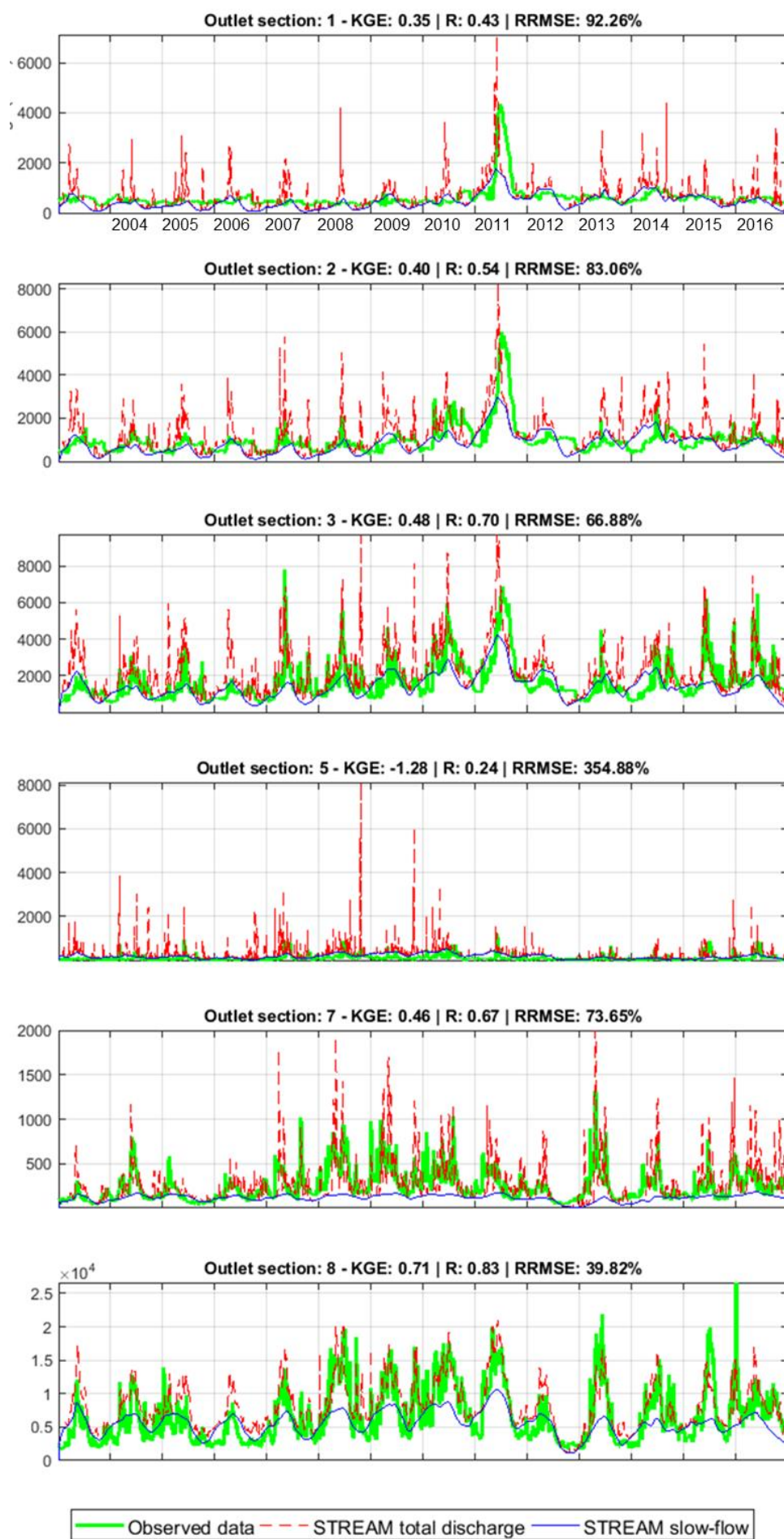
868 Figure 3. Mississippi sub-basin delineation. Red dots indicate the location of the discharge gauging
869 stations; different colours identify different inner sections (and the related contributing sub-basins)
870 used for the model calibration.
871



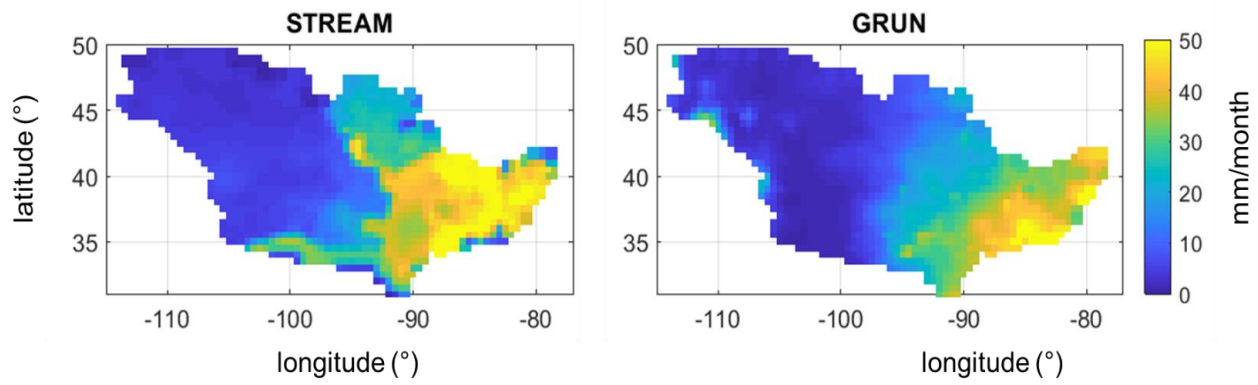
872

873 Figure 4. Comparison between observed and simulated river discharge time series over the five
 874 calibrated sections over Mississippi river basin. Performance scores at the top of each plot refer to
 875 the entire study period (2003–2016).

876



878
880 Figure 5. Comparison between observed and simulated river discharge time series over the gauged
881 sections not used in the calibration phase. Performance scores at the top of each plot refer to the entire
882 study period (2003–2016).
883



884

885 Figure 6. Mississippi river basin: mean monthly runoff for the period 2003–2014 obtained by
 886 STREAM [v1.3](#) and GRUN models.

887

APPENDIX

Table 1A. Description of STREAM v1.3 parameters, belonging module, variability range and unit.

<u>Parameter</u>	<u>Description</u>	<u>Module</u>	<u>Range Variability</u>	<u>Unit</u>
<u>C_m</u>	<u>degree-day coefficient</u>	<u>Snow</u>	<u>0.1/24-3</u>	<u>[-]</u>
<u>α</u>	<u>exponent of infiltration</u>	<u>Soil</u>	<u>1-30</u>	<u>[-]</u>
<u>T</u>	<u>characteristic time length</u>	<u>Soil</u>	<u>0.01-80</u>	<u>[days]</u>
<u>β</u>	<u>coefficient relationship slow runoff component and TWSA</u>	<u>Soil</u>	<u>0.1-20</u>	<u>[mm h⁻¹]</u>
<u>m</u>	<u>exponent in the relationship between slow runoff component and TWSA</u>	<u>Soil</u>	<u>1-15</u>	<u>[-]</u>
<u>γ</u>	<u>parameter of GIUH</u>	<u>Routing</u>	<u>0.5-5.5</u>	<u>[-]</u>
<u>C</u>	<u>Celerity</u>	<u>Routing</u>	<u>1-60</u>	<u>[km h⁻¹]</u>
<u>D</u>	<u>Diffusivity</u>	<u>Routing</u>	<u>1-30</u>	<u>[km² h⁻¹]</u>